Biochimica et Biophysica Acta 1838 (2014) 1430–1438

Contents lists available at ScienceDirect

Biochimica et Biophysica Acta

journal homepage: www.elsevier.com/locate/bbamem

# Trichoplaxin — A new membrane-active antimicrobial peptide from placozoan cDNA

Juraj Simunić [a], Dražen Petrov [b], Tahar Bouceba [c], Nédia Kamech [d,e], Monica Benincasa [f], Davor Juretić [a,*]

[a] Faculty of Science, University of Split, Nikole Tesle 12, 21000 Split, Croatia
[b] Max F. Perutz Laboratories, University of Vienna, Campus Vienna Biocenter, 1030 Vienna, Austria
[c] Université Pierre et Marie Curie — UPMC, Plateforme d'Interactions Moléculaires, Institut de Biologie Paris-Seine, IBPS, 7 Quai Saint-Bernard, 75252 Paris cedex 05, France
[d] Université Pierre et Marie Curie — UPMC, Equipe Biogenèse des signaux peptidiques, ER3, 7 Quai Saint-Bernard, Paris cedex 05, France
[e] Biology of Aquatic Organisms and Ecosystems (BOREA), UMR CNRS 7208 — UPMC — IRD207, Muséum National d'Histoire Naturelle, 7 rue Cuvier, CP32, 75231 Paris cedex 05, France
[f] Department of Life Sciences, University of Trieste, Via Giorgieri 5, 34127 Trieste, Italy

ARTICLE INFO

*Article history:*
Received 24 September 2013
Received in revised form 29 January 2014
Accepted 5 February 2014
Available online 12 February 2014

*Keywords:*
Antimicrobial peptide
EST database
*Trichoplax adhaerens*
Selectivity index
Surface plasmon resonance
Peptide–membrane interaction

ABSTRACT

A method based on the use of signal peptide sequences from antimicrobial peptide (AMP) precursors was used to mine a placozoa expressed sequence tag database and identified a potential antimicrobial peptide from *Trichoplax adhaerens*. This peptide, with predicted sequence FFGRLKSVWSAVKHGWKAAKSR is the first AMP from a placozoan species, and was named trichoplaxin. It was chemically synthesized and its structural properties, biological activities and membrane selectivity were investigated. It adopts an α-helical structure in contact with membrane-like environments and is active against both Gram-negative and Gram-positive bacterial species (including MRSA), as well as yeasts from the *Candida* genus. The cytotoxic activity, as assessed by the haemolytic activity against rat erythrocytes, U937 cell permeabilization to propidium iodide and MCF7 cell mitochondrial activity, is significantly lower than the antimicrobial activity. In tests with membrane models, trichoplaxin shows high affinity for anionic prokaryote-like membranes with good fit in kinetic studies. Conversely, there is a low affinity for neutral eukaryote-like membranes and absence of a dose dependent response. With high selectivity for bacterial cells and no homologous sequence in the UniProt, trichoplaxin is a new potential lead compound for development of broad-spectrum antibacterial drugs.



## 1. Introduction

Membrane selective peptides are a large and diverse group of membrane-active compounds including fusogenic, cell-penetrating, cytotoxic, self-associating integral membrane peptides and antimicrobial peptides, most of them exhibiting a characteristic activity spectrum and preference for certain types of biological membranes [1–4]. Antimicrobial peptides (AMPs) are gene coded molecules which are an essential part of the innate immune system, the first line of host defence in the early stages of exposure to pathogenic microorganisms [5]. AMPs are good candidates for natural selection to continuously modify existing sequences in response to the ever changing microbial biota. This makes them a remarkably diverse and ubiquitous group of molecules [6–11]. AMPs have been reported in all groups of living organisms, ranging from bacteria and fungi to plants and animals as parts of ancient antimicrobial defence system [12–15]. Given their molecular diversity and a mode of action different to that of conventional antimicrobials, it is not surprising that over the years the interest in AMPs as new potential lead compounds in drug development has continuously increased [16,17]. An added stimulus is the serious current problem of increasing bacterial resistance, combined with a dearth of novel molecular scaffolds for antibiotic development. In addition, it has been reported that many AMPs have a broader therapeutic potential as antiviral [18], antitumor [19], immunomodulating [20] or wound healing agents [21].

As antimicrobials, AMPs are part of a host defence strategy to fight infection based on a general disruption of the pathogen's cytoplasmic membrane. They can in fact create pores or lesions via carpet, barrel-stave or toroidal mechanisms [22]. This mode of action can be rapid and broad-spectrum, and is likely to be difficult for microorganisms to overcome. Indeed, for most AMPs there does not appear to be a single molecular target that could easily be modified as for conventional antibiotics, and the membrane modifications required to render AMPs ineffective are metabolically expensive for the pathogen. For this reason, AMPs may have a low propensity in inducing long-term resistance [23].

*Abbreviations:* AMP, antimicrobial peptide; $HC_{50}$, concentration for 50% haemolysis; $IC_{50}$, concentration for 50% of growth inhibition; LUVs, large unilamellar vesicles; MIC, minimum inhibitory concentration; MBC, minimal bactericidal concentration; PI, propidium iodide; TFE, trifluoroethanol; TB, trypan blue; SI, antimicrobial selectivity index; UniProt, Universal Protein Resource; DMPC, dimyristoylphosphatidylcholine; DMPG, dimyristoylphosphatidylglycerol

* Corresponding author at: Faculty of Science, University of Split, Nikole Tesle 12, 21000 Split, Croatia. Tel.: +385 21385286.
*E-mail address:* juretic@pmfst.hr (D. Juretić).

http://dx.doi.org/10.1016/j.bbamem.2014.02.003
0005-2736/

One of the principal difficulties in developing AMPs as antibiotics is their toxicity. This is often expressed as an insufficient selectivity when permeabilizing eukaryotic and prokaryotic cell membranes, making them too cytotoxic. Low selectivity is often reported as a high lytic activity towards erythrocytes in standard haemolytic assays. A range of theoretical and experimental methods has been developed in order to understand how to improve the membrane selectivity of natural occurring AMPs [24,25]. At the same time, the increasing abundance of new genetic information provided by genomic and expressed sequence tag (EST) sequencing could prove to be a rich source for identifying new peptides that natural selection has already shaped into therapeutically interesting candidates. The remarkable diversity of AMP sequences, even in closely related species, makes the direct mining of these rather difficult. On the other hand, the signal peptide regions in their precursors are well conserved [26–28], so that using these as query sequences has proven to be a valuable method for identifying new AMPs [29].

In this article we report a new, membrane-selective antimicrobial peptide that we named trichoplaxin. Its cDNA was identified in the EST database belonging to the placozoan *Trichoplax adhaerens*. Trichoplaxin-like sequences were not present in the UniProt data base. The peptide was chemically synthesized and its antimicrobial and haemolytic properties were established. Using model membrane systems we also studied its affinity for different membrane types in order to explain its biological properties that make this peptide potentially interesting for pharmacological applications.

## 2. Materials and methods

### 2.1. In silico analysis of sequences

Trichoplaxin precursor was first identified in the EST database by using a general method directed to finding novel AMPs by using signal peptides (SP) and propeptides of known AMPs developed by Petrov et al. (manuscript in preparation). A sequence similarity search was performed using the TBLASTN algorithm on the EST database with the signal peptide sequence (MKCATLFLVLSMVVLMAEPGDA) from the moronecidin (piscidin-1) precursor as query (GenBank Accession No. Q8UUG0). Although we have used many other AMP-associated SP as queries, the moronecidin SP proved to be a good choice before for finding novel AMPs with no homologues in the UniProt ([29] and Petrov et al. manuscript in preparation). We focused on one of the search results, namely the Trc_N-9_C14.t.scf *T. adhaerens* EST Library cDNA, with the code GI:295905054 and GenBank link gb|GR416833.1|. The following sequence was found in the 3′ 5′ Frame 1: *MKCAMIFLVLTLVVLMAEPGEC***FFGRLKSVWSAVKHGWKAAKSR**WRESKQSEQGEQAGQGGPPADQGQAPPNVAWR, with easily recognized signal peptide (italic letters) determined both by homology and using the SignalP server [30] (http://www.cbs.dtu.dk/services/SignalP/), a putative 22 residue long mature AMP (bold letters) determined by analogy to the antimicrobial peptide sequence of mature moronecidin (also 22 residues long), and a negatively charged propeptide at the C-terminus. Putative mature AMP was named trichoplaxin according to its annotation in the EST database.

All sequence alignments were done with ClustalW. Prediction of tridimensional structure was performed using the I-Tasser server [31] (http://zhanglab.ccmb.med.umich.edu/I-TASSER/) with default settings and visualized by YASARA View software (http://www.yasara.org/index.html). Prediction of molecular hydrophobicity potential was performed using the PLATINUM server [32] (http://model.nmr.ru/platinum/), while amphipathicity profile and preferences for membrane buried helical conformation were examined using SPLIT 4.0 server [33] (http://split4.pmfst.hr/split/4/). Helical wheel and wenxiang projections were performed with RZLab (http://rzlab.ucr.edu/scripts/wheel/wheel.cgi) and Wenxiang (http://www.jci-bioinfo.cn/wenxiang2) servers respectively.

### 2.2. Peptide synthesis and purification

The in silico predicted antimicrobial part of the trichoplaxin precursor sequence was synthesized using the solid phase FastMoc chemistry procedure on an Applied Biosystems 433A automated peptide synthesizer (Life technologies, Cergy-Pontoise, France) as described previously [24]. Resin and Fmoc-protected amino acids were purchased from Iris Biotech GMBH (Marktredwitz, Germany), and solvents from SDS-Carlo Erba (Vitry, France). Carboxamidated peptides were prepared on 4-methylbenzhydrylamine polystyrene resin (Fmoc-426 Rink Amide PEG MBHA PS resin) substituted at 0.51 mmol/g. Synthesis product was cleaved from the resin by a mixture of 95% trifluoracetic acid (TFA), 2.5% $H_2O$ and 2.5% Triisopropylsilan, precipitated in ether, centrifuged, and then lyophilized. The lyophilized crude peptides were purified by reversed-phase HPLC (RP-HPLC) on a Luna C18(2) column (10 μm, 10 × 250 mm from Phenomenex, Le Pecq, France), eluted at 5 ml/min with a 35–70% linear gradient of acetonitrile (ACN) 0.07% TFA in 0.1% TFA/water over 35 min. The homogeneity and identity of the synthetic peptides were assessed by MALDI-TOF mass spectrometry (Voyager DE-Pro, Applied Biosystems, Life technologies, Cergy-Pontoise, France) and analytical RP-HPLC on a Luna C18(2) column (5 μm, 4.6 × 250 mm) eluted at a flow rate of 0.75 ml/min by a 0–60% linear gradient of ACN 0.07% TFA in 0.1% TFA/water (1%/min).

### 2.3. Antimicrobial activity

*Minimum inhibitory concentration* (MIC) of trichoplaxin was determined by a standard microdilution method using 96-well microtiter cell culture plates. The tests were performed against Gram-positive and Gram-negative bacteria and yeasts (Gram-positive strains: *Staphylococcus aureus* ATCC 25923, *S. aureus* multiresistant ATCC BAA-44, *Enterococcus faecalis* ATCC 29212, *Listeria ivanovii*; Gram-negative strains: *Escherichia coli* ATCC 25922, *Pseudomonas aeruginosa* ATCC 27853, *Acinetobacter baumanii* ATCC 19606, *Klebsiella pneumoniae* ATCC 13883; yeast strains: *Candida albicans* ATCC 90028, *Candida parapsilosis* ATCC 22019). All bacteria except *L. ivanovii*, which was cultured in BHI medium, were cultured in LB medium and yeasts were cultured in YPD medium. Serial dilution of the peptide (50 μl) was incubated with 50 μl of $10^6$ cfu/ml of bacteria and yeasts, determined by absorbance at 600 nm and diluted in an appropriate liquid medium (Mueller-Hinton for all bacteria except *L. ivanovii* which was diluted in BHI broth; yeasts were diluted in YPD broth). Incubation of bacteria and yeasts was performed overnight (16 h) at 37 °C and 30 °C respectively. After incubation, the absorbance at 630 nm of each well was determined using a microplate reader (UVM340 ASYS, Eugendorf, Austria). The MIC was expressed as the lowest concentration of the peptide that completely inhibited bacterial growth and as the average value from three independent experiments, each performed in triplicate. Positive (0.7% formaldehyde) and negative ($H_2O$) inhibition controls and sterility control ($H_2O$) were also performed. Tests for bactericidal activity were performed by plating the bacterial suspension at MIC on solid medium and incubating overnight.

*Bacterial membrane permeabilization* was determined by flow cytometry, measuring the propidium iodide (PI) uptake by bacterial cells, as described in [34]. Analyses were performed with a Cytomics FC 5000 instrument (Beckman-Coulter, Inc., Fullerton, CA) equipped with an argon laser (488 nm, 5 mW) and using a photomultiplier tube fluorescence detector for orange filtered light (620 nm). All detectors were set on logarithmic amplification. Optical and electronic noises were eliminated by setting an electronic gating threshold on forward scattering detector, while the flow rate was kept at a data rate below 300 events/s to avoid cell coincidence. For each sample, at least 10,000 events were acquired and stored as list mode files. For the analyses, samples of $1 \times 10^6$ cells/ml were incubated in MH broth with the peptides at 37 °C for different times. PI (Sigma-Aldrich) was then added to the peptide-treated bacteria at a final concentration of

10 μg/ml, and the cells were analysed in the flow cytometer after 4 min incubation at 37 °C.

### 2.4. Cytotoxicity assays

*Haemolytic activity*: Peptide was diluted in a concentration range 1–800 μM and incubated in 96-well microtiter cell culture plates with $2 \times 10^7$ of washed rat erythrocytes (Charles River Laboratories, 465 L'Arbresle, France) in Dulbecco's phosphate-buffered saline, pH 7.4 (100 μl) for 1 h at 37 °C. After incubation the suspension was centrifuged (12,000 × g; 15 s) and the absorbance of supernatant was measured at 450 nm. A parallel incubation with 0.1% v/v Triton was performed to determine the absorbance value associated with 100% haemolysis. The $HC_{50}$ value was taken as the concentration of peptide producing 50% haemolysis.

*PI uptake*: Human leukemic U937 monocytes ($10^6$ cells/ml in PBS) were incubated with the fluorescent probe PI (10 μg/ml) and with different peptide concentrations ranging from 0.5 μM to 40 μM at 37 °C. Membrane damage was determined using the flow cytometer by monitoring the emission at 610 nm of PI intercalated to DNA after 5, 15, 30 and 45 min of peptide exposure. To evaluate the extent of permanent damage with respect to transient membrane permeabilization, peptide was removed after 30 min exposure by washing twice with PBS and cells were then resuspended in complete medium and incubated for additional 24 h. Uptake of PI to these cells was then measured by flow cytometry. For each measurement, 10,000 events were collected and stored as list mode files, which were then analysed using FCS Express 3 (DeNovo Software).

*MTT assay*: Breast cancer MCF7 cells were harvested from culture flasks after trypsinization, counted and appropriately diluted in complete medium ($0.5 \times 10^6$/ml); 100 μl of this cell suspension was transferred into each well of a 96-well culture plate. After overnight incubation, the supernatant was discarded and 0.5, 5, 10 and 25 μM concentrations of trichoplaxin were added in culture medium and incubated 24 h at 37 °C in a humidified atmosphere (5% $CO_2$). The colorimetric 3-(4,5-dimethylthiazol-2-yl)-2,5-diphenyl tetrazolium bromide (MTT) assay was then performed to assess the metabolic activity of treated cells in comparison to the untreated control. Briefly, 20 μl MTT solution (stock: 5 mg/ml) was added to each well, and cells were then incubated for 4 h at 37 °C. Finally, cells were lysed and MTT crystals solubilized with an isopropanol/0.04 M HCl solution. All measurements were carried out in triplicate on a microtiter plate reader (Tecan Männedorf, Switzerland) and the obtained data subjected to statistical analysis (Student–Newman–Keuls test) (GraphPad InStat).

### 2.5. Circular dichroism studies

The circular dichroism spectra were recorded at 20 °C using either a Jobin Yvon CD6 (Longjumeau, France) or a Jasco 700 (JASCO, Europe) spectropolarimeter. Spectra were recorded in quartz 1–2 mm path length cell between 185 and 260 nm with a spectral bandwidth of 2 and 0.5 nm steps. Peptide was tested at 30 μM in $H_2O$ (Milli-Q) in 10 or 80 mM sodium dodecyl sulfate (SDS) or 50% trifluoroethanol.

### 2.6. Preparation of large unilamelar vesicles

Two types of large unilamelar vesicles (LUVs) were prepared containing either only DMPC (dimyristoyl phosphatidylcholine) or DMPC/DMPG (dimyristoyl phosphatidylglycerol) mix. Briefly, for the preparation of DMPC vesicles 1.5 mg of DMPC (MW = 677.94 g/mol) was dissolved in 150 μl of chloroform. For DMPC/DMPG vesicles a mix of 3DMPC/DMPG, 1.12 mg of DMPC and 0.38 mg of DMPG (MW = 688.86 g/mol) was dissolved in 150 μl of methanol/chloroform (1:1). Tubes containing both lipid solutions were heated at 37 °C for 5 min in a bath and dried under the stream of nitrogen gas while rotating to form a thin layer of lipids and placed in a centrifugal evaporator at 45 °C during 3H to evaporate solvent traces. After evaporation the lipid mixtures were hydrated with 1.5 ml of filtered $Na_2HPO_4$ (10 mM), pre-heated at 37 °C, and mixed to obtain a homogeneous solution. This lipid solution contains multilamelar vesicles (MLV) which needed to be transformed into LUVs by seven cycles of freezing/thawing using liquid nitrogen and a bath at 37 °C respectively. This procedure will cause MLVs to burst their outer lipid layers leaving only LUVs in the solution. The lipid sample was filtered using an extruder (Avanti Polar Lipids, Inc.) preheated at 50 °C for 10 min with ten passages through filters of respectively reducing pore size (0.4, 0.2 and 0.1 μM). Final lipid solution (1 mg/ml) was kept in a clean vial at room temperature and used for subsequent analysis within 24 h.

### 2.7. Surface plasmon resonance analysis

Interaction between trichoplaxin and LUVs was measured using surface plasmon resonance (SPR) on a BIACORE 3000 instrument controlled by Biacore 3000 Control Software v4.1 (GE healthcare, Uppsala, Sweden) using the L1 chip support consisting of a carboxymethyl dextran matrix with additional hydrophobic alkane groups (GE healthcare). All experiments were done at 25 °C. Negative control experiment showed that the peptide interacted non-specifically with the L1 chip support (Fig. S1). In order to prevent these interactions BSA (bovine serum albumin 0.3 mg/ml; flow rate: 5 μl/min; contact time: 5 min) was first immobilized on L1 chip by hydrophobic interactions. This BSA treatment totally prevents peptide binding to the chip surface. Moreover, the peptide did not have any interaction with BSA molecules (Fig. S2). Then DMPC or DMPG/DMPC LUVs (DMPC LUVs: 0.2 mg/ml; flow rate: 1 μl/min; contact time: 5 min; DMPG/DMPC LUVs: 0.3 mg/ml, flow rate: 1 μl/min; contact time: 5 min) were immobilized by hydrophobic interactions. After this surface preparation, trichoplaxin binding experiments with DMPC or DMPG/DMPC were performed by diluting the peptide in HBS-N running buffer (HEPES 10 mM pH 7.4, NaCl 150 mM) (GE healthcare) and injecting on immobilized DMPC or DMPG/DMPC at a flow rate of 20 μl/min with a 1 min contact time. Finally, dissociation was performed under a

```
M. saxatilis moronecidin      MKCATLFLVLSMVVLMAEPGDAFFHHIFRG---IVHVGKTIHRLVTGGKAEQDQQDQQYQ 57
E. coioides epinecidin-1      MRCIALFLVLSLVVLMAEPGEGFIFHIIKG---LFHAGKMIHGLVTRRRHGVEELQDLDQ 57
P. americanus WF3             MKFTATFLVLSLVVLMAEPGECFLGALIKG---AIHGGRFIHGMIQ-NHHGYDEQQELNK 56
P. americanus WFYT            MKLAAAFLVLFLVVLMAEPGESFLGFLFHG---IRHGIKAIHGMIH-GN-SLDEMQELDK 55
T. adherens trichoplaxin      MKCAMIFLVLTLVVLMAEPGECFFGRLKSVWSAVKHGWKAAKSRWR-------ESKQSEQ 53
                              *:    **** :********:↑ putative mature peptide ↑        : .:  :

M. saxatilis moronecidin      QEQQEQQAQQYQRFN--RER--AAFD 79
E. coioides epinecidin-1      R-----------AFE--REKAFA--- 67
P. americanus WF3             R-----------AVD--E-------- 61
P. americanus WFYT            R-----------SFD--DNPNAIVFD 68
T. adherens trichoplaxin      G---EQAGQGGPPADQGQAPPNVAWR 76
                                          :
```

**Fig. 1.** Alignment of trichoplaxin precursor with antimicrobial peptide precursors from PFAM antimicrobial 12 family. Underlined — signal peptide; bold and arrows — putative trichoplaxin mature peptide.

**Table 1**
Antimicrobial activity of trichoplaxin against Gram-positive, Gram-negative bacteria and yeasts. Minimal inhibitory concentration (MIC), haemolytic activity ($HC_{50}$) and selectivity index (SI) are indicated.

| $HC_{50}$ (μM) | Bacterial strains[a] | | | | | | Yeast strains[b] | | |
|---|---|---|---|---|---|---|---|---|---|
| | GRAM+ | MIC (μM) | SI[c] (exp) | GRAM− | MIC (μM) | SI (exp) | Yeasts | MIC (μM) | SI (exp) |
| >800 | *S. aureus* | 3 | >260 | *E. coli* | 3–6 | >130 | *C. albicans* | 25 | >32 |
| | *S. aureus* (multires.) | 3 | >260 | *P. aeruginosa* | 6 | >130 | *C. parapsilosis* | 50 | >16 |
| | *L. ivanovii* | 3 | >260 | *A. baumanii* | 3 | >260 | | | |
| | *E. faecalis* | 12.5 | >65 | *K. pneumoniae* | 6 | >130 | | | |

[a] Gram-positive strains: *S. aureus* (ATCC 25923), multiresistant *S. aureus* (BAA-44), *E. faecalis* (ATCC 29212), *L. ivanovii*; Gram-negative strains: *E. coli* (ATCC 25922), *P. aeruginosa* (ATCC 27853), *A. baumanii* (ATCC 19606), *K. pneumoniae* (ATCC 13883).
[b] Yeast strains: *C. albicans* (ATCC 90028), *C. parapsilosis* (ATCC 22019).
[c] As the maximum haemolysis observed was 20% at 800 μM peptide, the SI = $HC_{50}$/MIC is likely to be considerably higher than the obtained value, as indicated.

20 μl/min flow during 5 min. The chip surface was regenerated using regeneration buffer (octyl-glucoside, 40 mM; flow rate: 5 μl/min; contact time: 1 min). For kinetic study different concentrations (50, 100, 150, 200 and 300 nM) of trichoplaxin were injected and their dose dependency response was measured. For general view of one injection cycle see Supplementary Data (Fig. S3). Data were analysed with BIAevaluation software 4.1 and the $K_D$ dissociation constant was determined using the Fit kinetic simultaneous $K_A/K_D$ (1:1 binding; Langmuir algorithm).

## 3. Results

### 3.1. In silico analysis of trichoplaxin

The trichoplaxin precursor, up to the acidic propeptide at its C-terminal, belongs to the 'Antimicrobial 12' family in the PFAM database (PF08107), which includes pleurocidin peptides from teleost fish. The four sequences with the lowest E-values for this AMP family belong to three fish species: *Epinephelus coioides*, *Morone saxatilis*, *Pseudopleuronectes americanus*, and are coding respectively for epinecidin-1, moronecidin, and pleurocidin-like peptides WF3 and WFYT (Fig. 1). Trichoplaxin precursor shows a remarkable similarity with pleurocidin peptides within its signal peptide region, with 77% sequence identity with *M. saxatilis* moronecidin. However, the complete precursor of trichoplaxin shares less than 40% identity with other pleurocidin family peptides, of which *P. americanus* WFYT has the highest score at 37% sequence identity. For trichoplaxin alone (bold sequence in Fig. 1) BLASTP cannot find anything similar in the database of non-redundant protein sequences up to the E-value of 6.8.

### 3.2. Trichoplaxin antimicrobial and haemolytic activities

Trichoplaxin was synthesized by FastMoc solid phase synthesis (see Section 2.2), and its antimicrobial activity was tested against several different bacterial and two yeast strains. The peptide showed similar activity against Gram-positive and Gram-negative strains (Table 1) with most values ranging from 3 to 12 μM. The lowest activity was against *E. faecalis* with a MIC at 12.5 μM. The same MIC (3 μM) was measured against both the antibiotic susceptible ATCC *S. aureus* strain and the multiresistant BAA-44 strain. The growth of two yeast strains, *C. albicans* and *C. parapsilosis* was inhibited with a MIC value of 25 μM and 50 μM respectively. Minimal bactericidal concentration (MBC) for all strains was determined to be at double the MIC value (data not shown).

A haemolytic activity assay was performed using rat erythrocytes (Table 1). The peptide was tested up to 800 μM where it produced 20% haemolysis of rat erythrocytes. It is therefore only possible to estimate a $HC_{20}$. It follows that the standard accepted definition for therapeutic or selectivity index SI = $HC_{50}$/MIC will give higher SI results. We estimate it to be over 100, depending on the organism (Table S1). Haemolytic activity however measures release of haemoglobin, a relatively large molecule, from cells. A more sensitive measure of host–cell membrane permeabilization is permeabilization to propidium iodide (PI). We carried out such an assay against U937 cells, a leukemic monocyte-derived cell line (Fig. 2A).

This assay indicated that while permeabilization was low at concentrations comparable to the MIC, a significant permeabilization occurred at 25 mM peptide. It should however be considered that PI is a small molecule, and can have alternative means of entering cells than membrane permeabilization [35]. For this reason we also carried out an MTT assay on breast cancer MCF7 cells, which is a generally accepted cytotoxicity assay (Fig. 2B). In this assay, also, cytotoxicity was low at concentrations comparable to the MIC, with the $IC_{20}$ being reached at 25 mM. Additionally, PI uptake after peptide treatment was evaluated also in bacteria. Both *E. coli* and *S. aureus* cells were tested (Fig. 3). The results indicate that at concentration close to MIC value (5 μM), trichoplaxin is permeabilizing *S. aureus* cells more readily than *E. coli* cells. After one hour incubation the percentage of PI positive cells is 10% and 33% for *E. coli* and *S. aureus* respectively. At concentration that is between two and three times the MIC value (25 μM), both *E. coli* and *S. aureus* cells are almost completely permeabilized (90%).

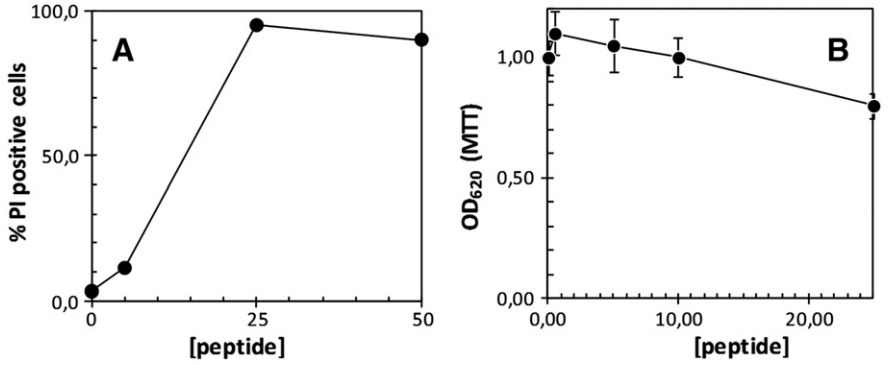


**Fig. 2.** Cytotoxic activity of trichoplaxin. A) Permeabilization of U937 cells at increasing concentrations of trichoplaxin (5 μM, 25 μM and 50 μM), estimated by flow cytometry, estimated as % permeabilized cells after incubation of $10^6$ cells with increasing concentrations of peptide for 1 h. B) MTT assay, carried out after incubation of $10^6$ MCF7 cells with increasing peptide concentrations (2.5 μM, 5 μM, 10 μM and 25 μM).

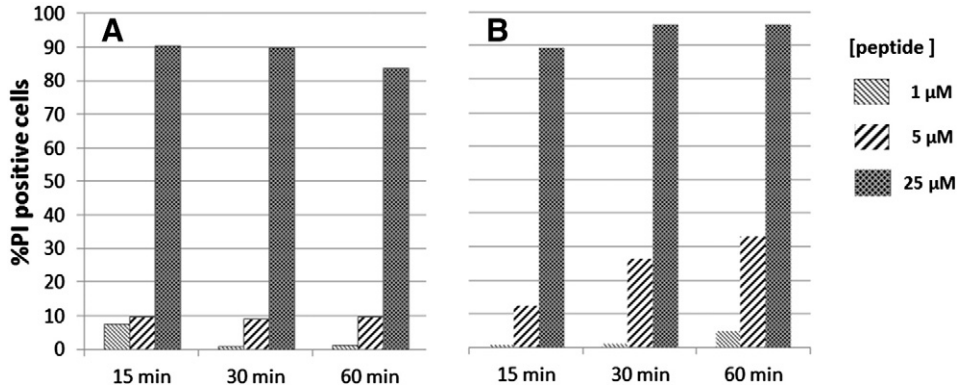


**Fig. 3.** Propidium iodide uptake of bacteria in contact with trichoplaxin. Permeabilization of *E. coli* (A) and *S. aureus* (B) after 1 h incubation with different concentrations (1 μM, 5 μM and 25 μM) of trichoplaxin.

Due to lack of similarity with mature teleost AMPs, the analogy with fish-derived mature antimicrobial peptide is not a strong argument for the cleavage site positioning peptide C terminal before third tryptophan of trichoplaxin precursor (Materials and methods section). In the case when third tryptophan is also considered to be inside mature trichoplaxin sequence (Fig. 1), an interesting pattern appears with aromatic residue at each seventh position: **FF**GRLKSV**W**SAVKHG**W**KAAKSR**W**R. This peptide was also synthesized and tested against *E. coli* and *S. aureus*. It showed a lower antimicrobial activity with MIC in the range of 25–50 μM (data not shown).

### 3.3. Structural studies

The spectra obtained by circular dichroism show (Fig. 4) solvent dependency of the secondary structure. In aqueous environment trichoplaxin has a minimum at 196 nm which indicates a disordered secondary structure. On the other hand, when placed in 80 mM SDS, the spectrum of the peptide changes with a single maximum at 191 nm and a strong minimum at 207 nm, with shoulders at 218 and 230 nm respectively. The position of the minimum is not compatible with a beta-sheet type structure. The spectrum has only partial resemblance to that of an alpha-helix as this has intense minima at 208 and 222 nm (Fig. 4A). Given the relatively high SDS concentration that was used, we lowered it to just above the micellar concentration (10 mM) to ensure that the spectral shape was not due to the latter. Under these conditions, the spectra were still not those expected for a canonical helical structure. On the other hand, when the CD spectrum was measured in trifluoroethanol, a solvent known to strongly induce a helical conformation, it had the typical shape of a helical peptide (Fig. 4B).

It is thus possible that trichoplaxin may have a structure that is not a canonical helix in a membrane-like environment, possibly due to the presence of four aromatic residues in the peptide sequence (F1, F2, W9 and W16), which may influence how trichoplaxin interacts with its environment.

Plotting trichoplaxin on a helical wheel projection reveals a secondary structure where residues are arranged in an amphipathic helical structure (Fig. 5A). An interruption of hydrophobic half of the amphipathic helix is caused by two arginine (R4 and R22) and a glycine (G15) residue. Prediction of tertiary structure based on homology with resolved PDB structures [31] suggests an α-helical structure with clearly visible amphipathic nature of the helix (Fig. 5B).

In order to examine the distribution of hydrophobicity across the length of the α-helix, we calculated the molecular hydrophobic potential [32] (MHP) of the peptide (Fig. 6). The 2D MHP map of the peptide surface shows that the hydrophobicity is concentrated around four residues, F1, F2, W9 and W16. As with helical wheel projection (Fig. 5A) the MHP map confirms the amphipathic character of the α-helix as hydrophobic patches created by these four residues are all in the right half of the map delineated by a vertical axis at 180° of rotation angle about the helix axis. Also, it is clearly visible that the hydrophobic property of the peptide is more prominent in its N-terminus, with most of hydrophobic patches placed in the lower half of the map, representing the first 11 residues of the peptide sequence.

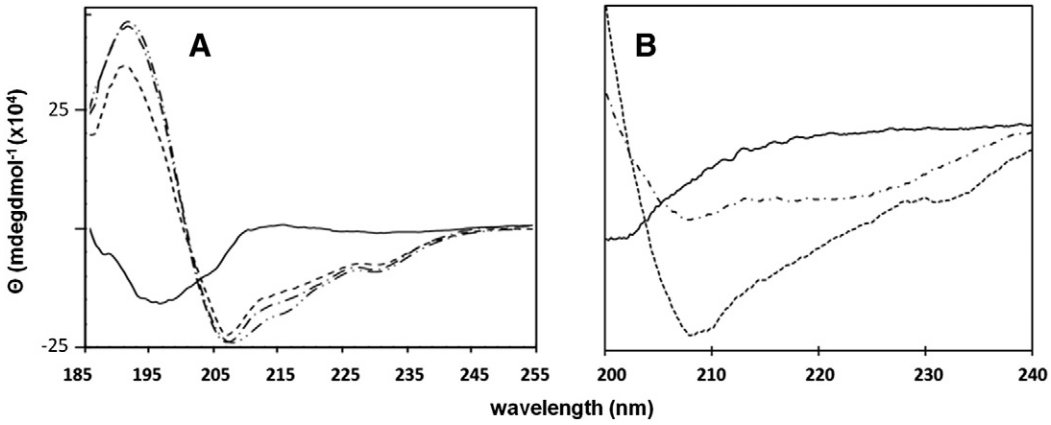


**Fig. 4.** Circular dichroism spectra of trichoplaxin. A) CD spectrum of trichoplaxin in water (——) and three different concentrations of the peptide in 80 mM SDS (30 μM - - - -; 50 μM – · – · – ; 100 μM – ·· – ·· –); B) CD spectrum of trichoplaxin at 30 μM in 10 mM sodium phosphate buffer (——) and in the presence of 10 mM SDS (- - - -) or 50% TFE (– · – · – · –). Spectra are the mean of at least three scans.

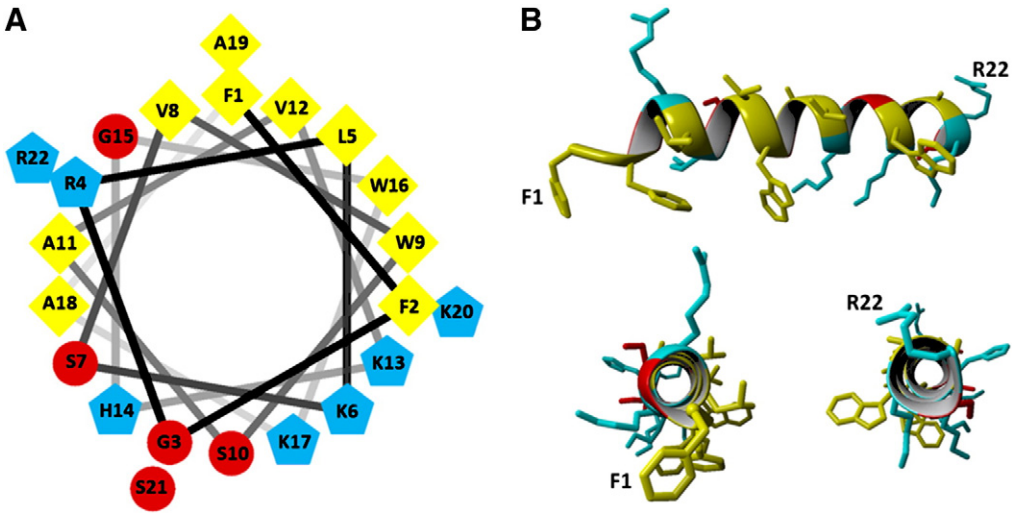


**Fig. 5.** Helical wheel projection of trichoplaxin (A) and predicted tertiary structure using I-TASSER server [31] and YASARA View software (B). Residues are colour and shape coded according to their hydrophobicity and charge. Nonpolar hydrophobic (yellow diamonds), polar uncharged (red circles) and polar basic (blue pentagons).

SPLIT server [33] also confirmed the amphipathic nature of predicted trichoplaxin helix and greater preference for membrane-buried helical conformation at the peptide hydrophobic N-terminal (data not shown).

### *3.4. Interaction assays of trichoplaxin with membrane models by surface plasmon resonance*

These assays were performed in order to measure the affinity of trichoplaxin towards two different types of membrane models, DMPC and DMPG/DMPC, a representation of eukaryotic and prokaryotic membranes respectively (Figs. 7 and 8). Interaction of the peptide with neutral DMPC vesicles was reversible with a signal dropping to zero spontaneously with the flow of running buffer after approximately 10 min (Fig. 7). This indicates that the peptide had a very low affinity for this type of vesicles and that it did not penetrate or bury in the lipid bilayer. Conversely, with the anionic DMPG/DMPC vesicles a spontaneous drop to zero of SPR signal was never achieved (Fig. 7), with a quantity of peptide attached to the vesicles remaining constant even after more than 50 min of continuous flow of running buffer. Kinetic tests using DMPG/DMPC LUVs showed that trichoplaxin has high affinity for this type of LUVs with a dissociation constant ($K_D$) of $8.65 \times 10^{-8}$ $s^{-1}$ and $\chi^2$ value of 2, showing a good fit (Fig. 8). A kinetic test using DMPC vesicles was unsuccessful as it was not possible to produce dose dependant results necessary for $K_D$ calculation (data not shown).

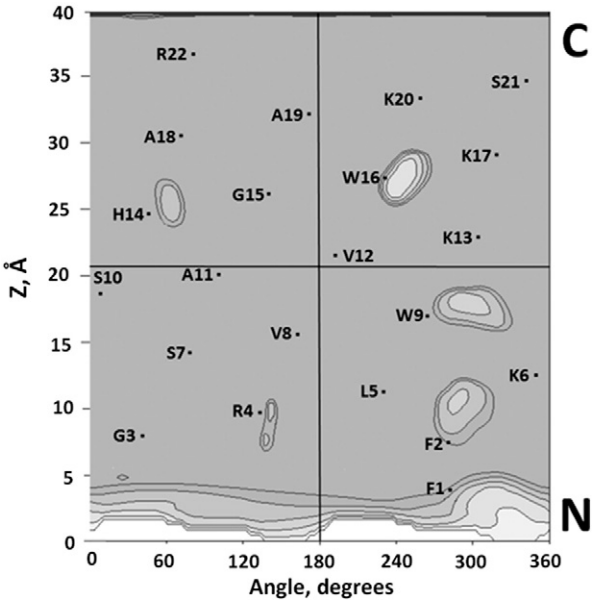


**Fig. 6.** The molecular hydrophobicity potential (MHP) on the surface of trichoplaxin as calculated by PLATINUM server [32]. MHP is given in octanol–water partition coefficient logP units. The value of the rotation angle about the helix axis and the rise along it are plotted on x and y axes respectively. Areas with MHP > 0.09 (lighter grey shades) are shown with contour intervals of 0.015. Dots next to residue symbols indicate the position of Cα atoms.

## 4. Discussion

The increasing efforts in both genome and EST sequencing have resulted in an abundance of potentially novel peptides with good therapeutic properties. In this study we give a first report of an antimicrobial peptide from the EST database of placozoan *T. adherens* found using as a query the signal peptide of a fish AMP piscidin. To the best of our knowledge no other AMP from placozoa has been identified so far. This peptide, apart from the preserved signal peptide, shares little similarity with known peptides from known fish species. A search in a draft version of *T. adherens* genome failed to produce a significant result but this may be due to the insufficiently completed sequencing of the genome. Additionally, phylum Placozoa, represented by extant species

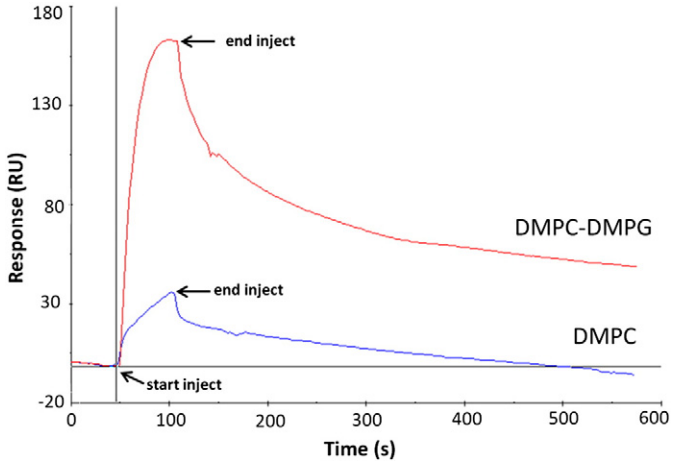


**Fig. 7.** Binding of trichoplaxin (0.5 μM) on DMPC (blue) and DMPG/DMPC (red) LUVs. Biacore sensograms showing the binding of trichoplaxin (0.5 μM) on DMPC (blue) or DMPG/DMPC (red) LUVs. Response is expressed in resonance units (RU) relative to time in seconds. Note the response due to end of injection of the peptide at 100 s.

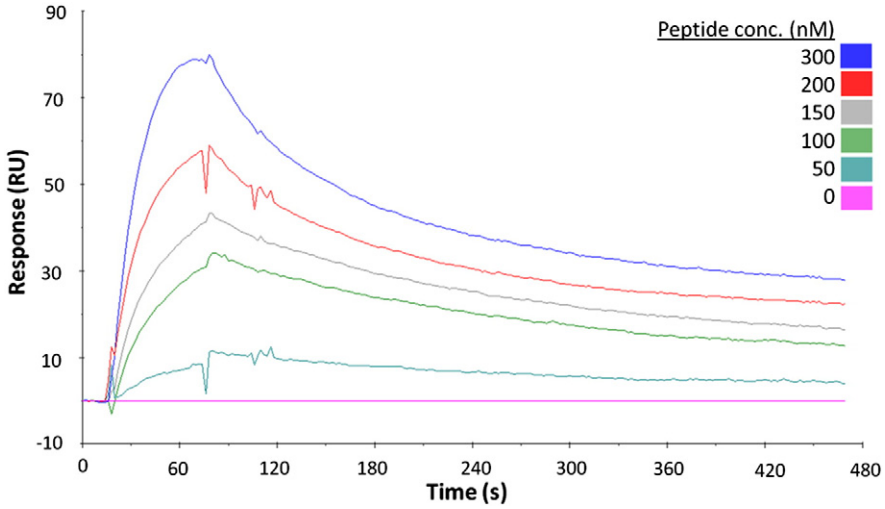


**Fig. 8.** Kinetic study of trichoplaxin binding to DMPG/DMPC large unilamelar vesicles. Five concentrations of trichoplaxin (50 to 300 nM) and HBS-N buffer were tested for their binding on DMPG/DMPC vesicles. The base line (in pink) corresponds to the HBS-N alone (see Materials and methods). Software analysis gives a $K_D$ value of $8.65 \times 10^{-8}$ M with a $\chi^2$ of 2 (see Materials and methods).

*T. adhaerens*, are often considered the simplest living animals [36]. Interestingly, these fragile animals, invisible in seawater, due to their small size, have strong chemical defence of unknown identity against other small animals [37]. In laboratory they feed on bacterial biofilms (green algae). Without having digestive organs or specialized cells, it is not clear how *T. adhaerens* manages to kill microbes for food or for its own defence. It has been noted that on the surface of the animal there is an abundance of vesicles of high lipid content that are known to expel their content to the surface upon external stimulation. However, the exact chemical composition of their content is still unknown [37].

The predicted antimicrobial part of the peptide was synthesized and a series of both structural and activity tests were performed. The CD spectra of trichoplaxin showed a slight shift in the second minimum of the curve, from 222 nm to 230 nm. This type of shift is not characteristic of either the α-helix or β-sheet and could be explained by four strongly absorbing aromatic residues in the sequence. However, in TFE the peptide does have a typical helical conformation but since TFE heavily promotes helical structure, it is not a definitive proof that trichoplaxin indeed is a typical α-helix. Aromatic residues mainly contribute to the absorption in the near-UV spectra (>250 nm) but when their frequency within the sequence is high, they can also contribute to the far-UV spectra, complicating the estimation of the secondary structure [38].

The biological activity of trichoplaxin was tested by antimicrobial test (MIC and MBC) against Gram-positive and Gram-negative bacteria and yeasts. Additionally, a haemolytic assay was performed. The peptide was equally active against Gram-positive and Gram-negative bacteria (3–6 μM) with the exception of Gram-positive *E. faecalis* (12 μM). On the other hand, PI uptake test showed a more pronounced permeabilization of *S. aureus* cells in comparison with *E. coli*. After 1 h of incubation, the percentage of permeabilized *S. aureus* cells was three times higher than the *E. coli* cells. The activity against two species of yeasts, *C. albicans* and *C. parapsilosis* was somewhat lower (25 and 50 μM respectively). In addition to being ubiquitously active against different microorganisms, trichoplaxin proved to have extremely good selectivity when looking at the haemolytic activity against rat erythrocytes with $HC_{50}$ value undetectable up to 800 μM of peptide concentration. With haemolysis rate of 20% at 800 μM we hypothesize that its $HC_{50}$ value is likely to be considerably higher than 1 mM. On the other hand, when we tested trichoplaxin for cell permeabilization by PI uptake and by MTT test, we found that peptide concentrations that produce cytotoxic effect in these experiments are much lower. PI uptake test shows significant cell permeabilizaton at 25 μM while MTT test predicts $IC_{50}$ in the range of 45–50 μM. These results taken together make it difficult to assess true cytotoxic activity of trichoplaxin since each test is placing it in a different concentration range. One of the explanations might be due to the nature of molecules that are taken as indicators of membrane damage. Since haemoglobin is a much larger molecule than PI it is possible that trichoplaxin is making pores of insufficient radius for haemoglobin to leak out of the erythrocyte, thus giving an impression of no cytotoxic activity. Also, as indicated in the work by Xhindoli et al. [35] PI can have alternative means of entry into the cell by activation of channel receptors which are not related to pore formation by the peptide. Taken together we believe that these results also raise the question of validity of generally accepted haemolytic tests as indicators of cytotoxicity and parameters for estimation of selectivity index in the field of antimicrobial peptide research. If measured by standard formula for selectivity index ($HC_{50}$/MIC), trichoplaxin has a SI value higher than 250 in some cases, which is one of the best results for known natural AMPs and their analogues that form α-helix in a membrane-like environment. The SI of three well-studied AMPs, PGLa, magainin-2 and magainin-2 analogue pexiganan is 105, 20, and 30 respectively, while their MIC against *E. coli* is 10, 50, and 1.5 μM respectively [39,40]. High selectivity of natural PGLa and magainin-2 peptides may be connected to their ability to make small short-living pores in bacterial-like membranes [4,41,42] so that similar mechanism of action can be proposed for the trichoplaxin.

Trichoplaxin selectivity was further tested using the surface plasmon resonance method. The peptide was tested for difference in interaction with two types of large unilamelar vesicles, representing prokaryotic-like negatively charged membranes (DMPG/DMPC) and eukaryotic-like, zwitterionic membranes (DMPC). In contact with (DMPG/DMPC) trichoplaxin acted in a predictable, dose dependant manner giving a dissociation constant $K_D$ of $8.65 \times 10^{-8}$ M. This $K_D$ is approaching the ones expressed by antigen–antibody interactions which are in the range of $10^{-9}$–$10^{-12}$ M. This is supported by the fact that the only means to remove the peptide from the chip was by washing the chip with 40 mM octyl-glucoside, removing both the peptide and the vesicles. Conversely, in the presence of DMPC vesicles the interaction of trichoplaxin changed dramatically, since after several attempts we were unable to produce a dose dependant response, with same concentrations of peptide giving different responses within the same series of injections. Additionally, the interaction of the peptide with this type of vesicles was weak enough to enable the complete and spontaneous dissociation of the peptide from the vesicles within several minutes.

This result supported the results obtained by haemolytic tests that showed a very low cytotoxicity.

Polyansky et al. [25] suggested that the haemolytic activity of α-helical peptides depends on hydrophobic properties of their N-terminus. For the example of latracins they demonstrated that a prominent N-terminal molecular hydrophobic potential (MHP) is characteristic for haemolytic peptides and that this toxic effect can be reduced by introducing substitutions with polar residues. Using their method we constructed a 2D MHP map of trichoplaxin (Fig. 6). Our results show that the peptide's high MHP values are concentrated primarily around four residues, F1, F2, W9 and W16. These regions are localized and do not form a wide hydrophobicity patch described for haemolytic peptides [25]. Also, the peptide seems to have more pronounced hydrophobic properties in the N-terminal region of the sequence with patches of high hydrophobicity concentrated mainly within the first ten residues of the sequence, around F1, F2 and W9 (Fig. 6). This characteristic could provide some insight in the action mechanism of the peptide as it could be that the N-terminal region is more critical in establishing interactions with the membrane [40].

Trichoplaxin has two arginines and two tryptophan residues in its sequence making it similar to the subset of AMPs called Arg-Trp rich peptides. Both intramolecular and intermolecular role of these two residue types in antimicrobial activity has been discussed in a previous work by Chan et al. [43]. Tryptophan has a complex electrostatic nature in its bulky side chain due to significant quadrupole moment of the indole ring. It has a π–electron system with negatively charged clouds and it can take part in cation–π interactions [44]. While in the interfacial region of lipid bilayer, tryptophan can form hydrogen bonds with both water and charged components of the lipid bilayer and its bulky side chain is in an energetically more favourable environment than it would be residing deeper within the cohesive hydrophobic acyl chain environment of the lipid bilayer [45]. Thus, tryptophan is a suitable amino acid to enable the peptide's prolonged association with the membrane. Arginine on the other hand with its cationic nature provides means for electrostatic interaction with target membranes and it can form hydrogen bonds with negatively charged parts of the membrane such as LPS, teichoic acid, or phosphatidyl glycerol phospholipid headgroups. Also, if interacting with tryptophan, arginine can have its charge shielded, allowing for an easier penetration into the lipid bilayer [44]. The cation–π interactions are however possible between all aromatic amino acids and both arginine and lysine [46]. Intermolecular interactions of lysines and spatially close aromatic residues are feasible in trichoplaxin, as indicated by helical wheel (Fig. 5) and wenxiang diagram (Fig. 9) [47].

Trichoplaxin has four connected small motifs of the type [G,A,S]XXX[G,A,S], where X is any amino acid, known to promote self-association and interaction of helical peptides in a membrane environment [48]. These are underlined motifs: FF**G**RLK**S**VWS**A**VKH**G**WKA**A**KSR. It remains to be explored how unique pattern of small motifs, amphipathicity, hydrophobicity and preferences profile for membrane-buried helix [32,33], in addition to possible cation–π interactions and combination of electrostatic and hydrophobic interactions with membrane components, brings about trichoplaxin exquisite ability to select between bacterial-like and eukaryotic-like membranes.

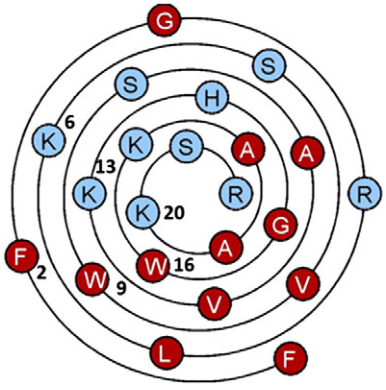


**Fig. 9.** Wenxiang diagram of trichoplaxin. Red — hydrophobic residues; Blue — polar residues. Potential cation–π interactions: F2-K6, W9-K13, W16-K20.

## 5. Conclusions

In this study we report a first antimicrobial peptide from *T. adhaerens* EST database, named trichoplaxin. Our results demonstrate that this peptide has a good activity against Gram − and Gram + bacteria, including drug-resistant strains, and a very low haemolytic activity. Surface plasmon resonance experiments suggest that the peptide low toxicity is related to its electrostatic and hydrophobic interactions with membrane phospholipids. High selectivity index and broad activity spectrum make trichoplaxin a good candidate for further investigation of peptides that could find their way to the clinical use.

## Acknowledgements

We would like to thank Dr. Christophe Piesse (Université Pierre et Marie Curie) for the peptide synthesis, Dr. Sabrina Pacor for help in setting up the cytotoxicity experiments and Dr. Alessandro Tossi (University of Trieste) for constructive discussions during preparation of this manuscript. This work was partly supported by the Croatian Ministry of Science, Education and Sports grant (177-1770495-0476 to DJ) and by a grant of French government to JS.

## Appendix A. Supplementary data

Supplementary data to this article can be found online at http://dx.doi.org/10.1016/j.bbamem.2014.02.003.

## References

[1] L. Lins, M. Decaffmeyer, A. Thomas, R. Brasseur, Relationships between the orientation and the structural properties of peptides and their membrane interactions, Biochim. Biophys. Acta 1778 (2008) 1537–1544.
[2] B. Bechinger, C. Aisenbrey, The polymorphic nature of membrane-active peptides from biophysical and structural investigations, Curr. Protein Pept. Sci. 13 (2012) 602–610.
[3] K. Splith, I. Neundorf, Antimicrobial peptides with cell-penetrating peptide properties and vice versa, Eur. Biophys. J. 40 (2011) 387–397.
[4] T. Tachi, R.F. Epand, R.M. Epand, K. Matsuzaki, Position-dependent hydrophobicity of the antimicrobial magainin peptide affects the mode of peptide–lipid interactions and selective toxicity, Biochemistry 41 (2002) 10723–10731.
[5] G. Diamond, N. Beckloff, A. Winberg, K.O. Kisch, The roles of antimicrobial peptides in innate host defense, Curr. Pharm. Des. 15 (2009) 2377–2392.
[6] A. Tossi, L. Sandri, A. Gianspero, Amphipatic, α-helical antimicrobial peptides, Biopolymers 55 (2000) 4–30.
[7] M. Novković, J. Simunić, V. Bojović, A. Tossi, D. Juretić, DADP: the database of anuran defense peptides, Bioinformatics 28 (2012) 1406–1407.
[8] G. Wang, X. Li, Z. Wang, APD2: the updated antimicrobial peptide database and its application in peptide design, Nucleic Acids Res. 37 (2009) D933–D937.
[9] R. Hammami, J. Ben Hamida, G. Vergoten, I. Fliss, PhytAMP: a database dedicated to antimicrobial plant peptides, Nucleic Acids Res. 37 (2009) D963–D968.
[10] R. Hammami, A. Zouhir, J. Ben Hamida, I. Fliss, BACTIBASE: a new web-accessible database for bacteriocin characterization, BMC Microbiol. 7 (2007) 89.
[11] L. Whitmore, B.A. Wallace, The Peptaibol Database: a database for sequences and structures of naturally occurring peptaibols, Nucleic Acids Res. 32 (2004) D593–D594.
[12] M. Nishie, J.I. Nagao, K. Sonomoto, Antimicrobial peptides "bacteriocins": an overview of their diverse characteristics and applications, Biocontrol Sci. 1 (2012) 1–16.
[13] M. Hajji, K. Jellouli, N. Hmidet, R. Balti, A. Sellami-Kamoun, M. Nasri, A highly thermostable antimicrobial peptide from *Aspergillus clavatus* ES1: biochemical and molecular characterization, J. Ind. Microbiol. Biotechnol. 8 (2010) 805–813.
[14] H.U. Stotz, J.G. Thomson, Y. Wang, Plant defensins: defense, development and application, Plant Signal. Behav. 4 (2009) 1010–1012.
[15] M. Zasloff, Antimicrobial peptides of multicellular organisms, Nature 415 (2002) 389–395.
[16] A.T. Yeung, S.L. Gellatly, R.E. Hancock, Multifunctional cationic host defence peptides and their clinical applications, Cell. Mol. Life Sci. 68 (2011) 2161–2176.
[17] F.P. da Silva, M.C.C. Machado, Antimicrobial peptides: clinical relevance and therapeutic implications, Peptides 36 (2012) 308–314.

[18] R. Lai, Y.T. Zheng, J.H. Shen, G.J. Liu, H. Liu, W.H. Lee, S.Z. Tang, Y. Zhang, Antimicrobial peptides from skin secretions of Chinese red belly toad *Bombina maxima*, Peptides 3 (2002) 427–435.
[19] H. van Zoggel, Y. Hamma-Kourballi, C. Galanth, A. Ladram, P. Nicolas, J. Courty, M. Amiche, J. Delbé, Antitumor and angiostatic peptides form frog skin secretions, Amino Acids 42 (2012) 385–395.
[20] A. Di Nardo, M.H. Braff, K.R. Taylor, C. Na, R.D. Granstein, J.E. McInturf, S. Krutzik, R.L. Modlin, R.L. Gallo, Cathelicidin antimicrobial peptides block fendritic cell TLR4 activation and allergic contact sensitization, J. Immunol. 178 (2007) 1829–1834.
[21] J.D. Heilborn, M.F. Nilsson, G. Kratz, G. Weber, The cathelicidin anti-microbial peptide LL-37 is involved in re-epithelization of human skin wounds and is lacking in chronic ulcer epithelium, J. Invest. Dermatol. 120 (2003) 379–389.
[22] Y. Park, K.S. Hahm, Antimicrobial peptides (AMPs): peptide structure and mode of action, J. Biochem. Mol. Biol. 38 (2005) 507–516.
[23] A.K. Marr, W.J. Gooderham, R.E. Hancock, Antibacterial peptides for therapeutic use: obstacles and realistic outlook, Curr. Opin. Pharmacol. 6 (2006) 468–472.
[24] N. Kamech, D. Vukičević, A. Ladram, C. Piesse, J. Vasseur, V. Bojović, J. Simunić, D. Juretić, Improving the selectivity of antimicrobial peptides from anuran skin, J. Chem. Inf. Model. 12 (2012) 3341–3351.
[25] A.A. Polyansky, A.A. Vassilievski, P.E. Volynsky, O.V. Vorontsova, O.V. Samsonova, N.S. Egorova, N.A. Kyrolov, A.V. Feofanov, A.S. Arseniev, E.V. Grishin, R.G. Efremov, N-terminal amphipatic helix as a trigger of haemolytic activity in antimicrobial peptides: a case study in latracins, FEBS Lett. 583 (2008) 2425–2428.
[26] P. Nicolas, D. Vanhoye, M. Amiche, Molecular strategies in biological evolution of antimicrobial peptides, Peptides 24 (2003) 1669–1680.
[27] E. König, O.R. Bininda-Emonds, Evidence for convergent evolution in the antimicrobial system in anuran amphibians, Peptides 32 (2011) 20–25.
[28] G.M. Morrison, C.A.M. Semple, F.M. Kilanowski, R.E. Hill, J.R. Dorin, Signal sequence conservation and mature peptide divergence within subgroups of the murine β-defensin gene family, Mol. Biol. Evol. 20 (2003) 460–470.
[29] V. Tessera, F. Guida, D. Juretić, A. Tossi, Identification of antimicrobial peptides from teleosts and anurans in expressed sequence tags databases using conserved signal sequences, FEBS J. 279 (2012) 724–736.
[30] T.N. Petersen, S.B. Gunnar von Heijne, H. Nielsen, SignalP 4.0: discriminating signal peptides from transmembrane regions, Nat. Methods 8 (2011) 785–786.
[31] Y. Zhang, I-TASSER server for protein 3D structure prediction, BMC Bioinforma. 9 (2008), http://dx.doi.org/10.1186/1471-2105-9-40.
[32] T.V. Pyrkov, A.O. Chuganov, N.A. Krylov, D.E. Nolde, R.G. Efremov, PLATINUM: a web tool for analysis of hydrophobic/hydrophilic organization of biomolecular complexes, Bioinformatics 25 (2009) 1201–1202.
[33] D. Juretic, L. Zoranic, D. Zucic, Basic charge clusters and predictions of membrane protein topology, J. Chem. Inf. Comput. Sci. 42 (2002) 620–632.
[34] E. Podda, M. Benincasa, S. Pacor, F. Micali, M. Mattiuzzo, R. Gennaro, M. Scocchi, Dual mode of action of Bac7, a proline-rich antibacterial peptide, Biochim. Biophys. Acta 1760 (2006) 1732–1740.
[35] D. Xhindoli, S. Pacor, F. Guida, N. Antcheva, A. Tossi, Native oligomerization determines the mode of action and biological activities of human cathelicidin LL-37, Biochem. J. 457 (2014), http://dx.doi.org/10.1042/BJ20131048.
[36] M. Srivastava, E. Begovic, J. Chapman, N.H. Putnam, U. Hellsten, T. Kawashima, A. Kuo, T. Mitros, A. Salamov, M.L. Carpenter, A.Y. Signorovitch, M.A. Moreno, K. Kamm, J. Grimwood, J. Schmutz, H. Shapiro, I.V. Grigoriev, L.W. Buss, B. Schierwater, S.L. Dellaporta, D.S. Rokhsar, The *Trichoplax* genome and the nature of placozoans, Nature 454 (2008) 955–960.
[37] V.B. Pearse, O. Voigt, Field biology of placozoans (Trichoplax): distribution, diversity, biotic interactions, Integr. Comp. Biol. 47 (2007) 677–692.
[38] D.H.A. Corrêa, C.H.I. Ramos, The use of circular dichroism spectroscopy to study protein folding, form and function, Afr. J. Biochem. Res. 3 (2009) 164–173.
[39] L.M. Gottler, A. Ramamoorthy, Structure, membrane orientation, mechanism, and function of pexiganan — a highly potent antimicrobial peptide designed from magainin, Biochim. Biophys. Acta 1788 (2009) 1680–1686.
[40] D. Juretić, D. Vukičević, N. Ilić, N. Antcheva, A. Tossi, Computational design of highly selective antimicrobial peptides, J. Chem. Inf. Model. 49 (2009) 2873–2882.
[41] K. Matsuzaki, Control of cell selectivity of antimicrobial peptides, Biochim. Biophys. Acta 1788 (2009) 1687–1692.
[42] K. Matsuzaki, Magainins as paradigm for the mode of action of pore forming polypeptides, Biochim. Biophys. Acta 1376 (1998) 391–400.
[43] D.I. Chan, E.J. Prenner, H.J. Vogel, Tryptophan- and arginine-rich antimicrobial peptides: structures and mechanisms of action, Biochim. Biophys. Acta 1758 (2006) 1184–1202.
[44] D.A. Dougherty, Cation–pi interactions in chemistry and biology: a new view of benzene Phe, Tyr, and Trp, Science 271 (1996) 163–168.
[45] W.M. Yau, W.C. Wimley, K. Gawrisch, S.H. White, The preference of tryptophan for membrane interfaces, Biochemistry 37 (1998) 14713–14718.
[46] J.P. Gallivan, D.A. Dougherty, Cation–π interactions in structural biology, Proc. Natl. Acad. Sci. U. S. A. 96 (1999) 9459–9464.
[47] K.C. Chou, W.Z. Lin, X. Xiao, Wenxiang: a webserver for drawing wenxiang diagrams, Nat. Sci. 3 (2011) 862–865.
[48] A. Senes, M. Gerstein, D.M. Engelman, Statistical analysis of amino acid patterns in transmembrane helices: the GxxxG motif occurs frequently and in association with β-branched residues at neighboring positions, J. Mol. Biol. 296 (2000) 921–936.